Experimental Investigation of the Effect of Injected Interstitials on Void Formation

B. Badger, Jr., D.L. Plumton, S.J. Zinkle, R.L. Sindelar, G.L. Kulcinski, R.A. Dodd and W.G. Wolfer

June 1984

UWFDM-582

Presented at the 12th Intern. Symposium on the Effects of Radiation on Materials, Williamsburg, VA, June 18-20, 1984; to be published in ASTM (1984).

FUSION TECHNOLOGY INSTITUTE

UNIVERSITY OF WISCONSIN

MADISON WISCONSIN

Experimental Investigation of the Effect of Injected Interstitials on Void Formation

B. Badger, Jr., D.L. Plumton, S.J. Zinkle, R.L. Sindelar, G.L. Kulcinski, R.A. Dodd and W.G. Wolfer

Fusion Technology Institute
University of Wisconsin
1500 Engineering Drive
Madison, WI 53706

http://fti.neep.wisc.edu

June 1984

UWFDM-582

Presented at the 12th Intern. Symposium on the Effects of Radiation on Materials, Williamsburg, VA, June 18-20, 1984; to be published in ASTM (1984).

EXPERIMENTAL INVESTIGATION OF THE EFFECT OF INJECTED INTERSTITIALS ON VOID FORMATION

B. Badger, Jr., D.L. Plumton, S.J. Zinkle,
R.L. Sindelar, G.L. Kulcinski,
R.A. Dodd, W.G. Wolfer

Fusion Engineering Program
Nuclear Engineering Department
University of Wisconsin-Madison
Madison, WI 53706

June 1984

UWFDM-582

EXPERIMENTAL INVESTIGATION OF THE EFFECT OF INJECTED INTERSTITIALS ON VOID FORMATION

B. Badger, Jr., D.L. Plumton, S.J. Zinkle, R.L. Sindelar, G.L. Kulcinski, R.A. Dodd, and W.G. Wolfer

Fusion Engineering Program, Nuclear Engineering Department
University of Wisconsin, 1500 Johnson Drive
Madison, WI 53706

Abstract

Pure nickel, a "pure" 316-type stainless steel (P7) and two high strength copper alloys have been irradiated with either 14-MeV nickel or copper ions to a peak damage level of 50 dpa (K = 0.8) at homologous temperatures ranging from 0.4 to 0.6 Tm. The irradiated foils have been examined in cross section in an electron microscope. The injected interstitial effect on the suppression of the measured void densities in Ni and P7 was found to increase with decreasing temperature. The comparison of these results with nucleation theory shows good qualitative agreement. Quantitative discrepancies are attributed to diffusional spreading of point defects and to the presence of impurity atoms in the matrix. A copper alloy irradiated at 300°C showed a small heterogeneous void density characteristic of the high temperature end of the void swelling regime, while no voids formed in the alloys irradiated ≥ 400°C. This result is in excellent agreement with nucleation theory which indicates the void swelling regime in ion-irradiated, low impurity copper should be less than 300°C (0.42 Tm).

Key Words: copper alloys, nickel, stainless steel, ion irradiation, void formation, TEM, injected interstitials, void nucleation theory, diffusional spreading

Introduction

During the past decade many radiation effects studies have utilized heavy ions to produce displacement damage in metals. Heavy ion irradiation offers the advantage of rapid accumulation of displacement damage as compared to neutron irradiation. However, differences in the displacement cascade structure and displacement rates between ion and neutron irradiations, along with the absence of transmutation products in ion irradiations, make it difficult to establish correlations between the damage resulting from the two types of irradiations. An additional factor which has received somewhat less attention is that heavy ion irradiation deposits the irradiating ion in the matrix in the form of an excess interstitial. This injected ion effect was originally assumed to be minimal, but has subsequently been found to significantly reduce void formation and growth under the appropriate conditions.

Where point defect recombination is dominant, the injected interstitials can reduce the void growth rate. This effect was predicted by Brailsford and Mansur [1] and experimentally verified by Lee et al. [2]. The reduction is significant when the bias is small, i.e. when the current of vacancies is almost equal to the current of interstitials into the void. Obviously this is the case for voids of the critical size. Therefore, it may be expected that the injected interstitials will affect void nucleation to a greater extent than void growth. Plumton and Wolfer [3] have recently shown that void nucleation can be suppressed by the presence of the injected ions.

An injected ion comes to rest in the matrix as an interstitial without a vacancy partner. Therefore, there exists an excess number of interstitials in the region where the ions are deposited. In a heavy ion irradiation the peak in the damage profile overlaps the ion deposition profile, meaning that there

is an excess of interstitials in the damage peak. These excess interstitials may perturb the balance between the vacancy and interstitial flux to the void nuclei, causing suppression of void nucleation. Since the excess interstitials are a small fraction of the total interstitial concentration, they are only important when most of the point defects produced by displacements are recombining. The effect of the injected ions on void nucleation should therefore become increasingly important at lower temperatures. Garner [4] recently reevaluated previous work in light of this suppression effect and found that in various metals injected interstitials may have a pronounced effect on experimental void swelling results.

For high energy ions, in contrast to low energy ions [3,5], there exists a region midway along the range that is not affected by either the front surface or by the injected ions. The development of the cross section procedure for post-irradiation examination allows void swelling data for different displacement rates and fluences to be obtained from one sample [6-9]. Transmission electron microscopy (TEM) observations over the entire damage range allows a determination to be made of the effect of injected interstitials on void formation. The cross section technique is now well-established for nickel [6], copper [7], and stainless steel [8,9].

Pure nickel, a "pure" 316-type stainless steel (P7), and 2 high strength copper alloys have been irradiated with either 14-MeV nickel or copper ions. These samples have been electroplated with nickel or copper and thinned to observe the damage region in cross section. The use of 3 different metallic systems allows an assessment to be made of the general influence of injected ions on void nucleation. The irradiations were conducted at homologous

temperatures ranging from 0.4 Tm to 0.6 Tm in order to determine the effect of temperature on the suppression of void formation in the peak damage region.

Experimental Procedure

The composition and impurity content of the "pure" 316-type stainless steel alloy P7, nominally Fe-17Cr-16.7Ni-2.5Mo, [9,10] and AMZIRC (Cu-0.15Zr) and AMAX-MZC (Cu-0.6Cr-0.15Zr-0.05Mg) copper alloys [11] are given elsewhere. The purity of the nickel used in this investigation was 0.99995. The pre-irradiation preparation of all three materials involved successive mechanical polishing operations down to an abrasive of 0.3 μm alumina powder. In addition, the copper alloys and pure nickel samples were electropolished to remove any cold work from the mechanical polish.

The materials were irradiated at the University of Wisconsin Heavy-Ion Irradiation Facility using 14-MeV Ni^{3+} ions for the P7 alloy and pure nickel samples and 14-MeV Cu^{3+} ions for the copper alloys. Table 3 lists the irradiation parameters used in this study.

Post-irradiation preparation for TEM analysis involved a cross-section technique described elsewhere for the pure nickel [6], the copper alloys [7] and P7 alloy [9]. These procedures allow the entire damage region of the heavy ions to be analyzed for a single irradiated sample. TEM was performed using a JEOL TEMSCAN-200CX electron microscope.

Theoretical Parameters and Procedures

Comparisons between materials with varying amounts of irradiation-induced displacement damage are usually done in terms of displacements per atom, DPA. This value is obtained by use of a modified Kinchen and Pease model [12], so that the number of displacements (R_D) is given by

$$R_D = \frac{\phi\ K\ S_D(x)}{2\ \rho\ E_D}$$

where ϕ is the fluence, ρ is the atomic density, E_D is the effective displacement energy and $S_D(x)$ is the energy available for displacements at a depth x (damage energy). The last parameter, K, is the displacement efficiency which Torrens and Robinson took to be 0.8, which has been used as a standard value over the years for DPA calculations. Recent experimental and theoretical studies on the displacement efficiency have revealed that it is strongly dependent on energy, with K decreasing for increasing recoil energy (see Ref. 13 for a review). These results indicate that for high energy ($\gtrsim$ 1 MeV) neutron or heavy ion irradiations of fcc metals the efficiency is ~ 0.3, which reduces many previously cited damage values by a factor of 3/8. The defect production efficiency used in this paper for the determination of DPA rate and excess interstitial fraction (ε_i) is K = 0.3.

The Brice code [14] has been used to calculate the damage rates and excess interstitial fractions for 14-MeV Cu or Ni ions incident on copper, nickel or stainless steel. The excess interstitial fraction, ε_i, taken as the ratio of deposited ions to the interstitials produced by damage that survive cascade recombination is also affected by the efficiency. ε_i is taken as

$$\varepsilon_i = \frac{f(x)\ \phi}{E_{ff}\ \rho\ R_D}$$

where f(x) is the deposited ion distribution function at a depth x and E_{ff} is the fraction of defects that escape in-cascade recombination. Therefore, while previous damage rates scale by 3/8, previous excess interstitial frac-

tions scale by 8/3. The effective displacement energies used for the Cu, Ni and P7 stainless steel damage calculations are 29, 40 and 32 eV respectively.

The steady state void nucleation theory for heavy ion irradiations presented by Plumton and Wolfer [3] is used here along with the modification of a vacancy surface sink term previously included [5] in the nucleation computer code. The materials parameters, Table 1, used in the nucleation calculations are experimentally determined values taken from the literature. An attempt has been made to qualitatively match the theoretical output with the experimental results. The matching is accomplished by slightly modifying some of the input materials parameters listed in Table 1. The materials values that have been used to adjust the theoretical nucleation profiles are the energies and entropies of vacancy migration and formation (E_v^m, E_v^f, S_v^m, S_v^f), the surface energy of the metal (γ) and the void bias factors (Z_i^o, Z_v^o) for interstitial and vacancy capture. The adjustment consists of matching the theoretical nucleation rate with the experimentally determined void density. The experimental void density is assumed to be the density that is reached after nucleation has stopped so that the nucleation period must be less than the total irradiation time. A nucleation rate of $\sim 10^{18} - 10^{19}$ voids/m^3/s was obtained from measured void densities of $10^{20} - 10^{22}$ voids/m^3 and total irradiation times of $\sim 10^3$ s.

The vacancy diffusivity (D_v) and thermal equilibrium concentration (C_v^{eq}) were determined in accordance with the formalism of Seeger and Mehrer [15] for the self-diffusion coefficient (D_{SD}):

$$D_{SD} = (D_v)(C_v^{eq}) = a^2 \upsilon_o e^{\frac{S_v^m + S_v^f}{k}} e^{-\left(\frac{E_v^m + E_v^f}{kT}\right)} \qquad (1)$$

where the jump frequency for FCC crystals ν_o is $\frac{1}{a}\sqrt{E_v^m/M}$, a is the lattice parameter and M is the average mass of the atoms making up the lattice. Experimental self-diffusion data only allows the sums $S_v^m + S_v^f$ and $E_v^m + E_v^f$ to be determined. Therefore a decrease in S_v^f or E_v^m implies an increase in S_v^m or E_v^f. A complete parametric study of varying the energies and entropies of vacancy migration and formation and determining the impact on void nucleation is beyond the scope of this paper. However, several trends have been noticed as these input parameters are modified. Raising E_v^f or lowering S_v^f increases the nucleation rate, most noticeably at high temperatures, while the effect of the injected interstitials on void nucleation suppression is decreased.

The vacancy energies and entropies for copper and nickel have been extensively examined in the literature. For copper the self-diffusion data is well determined. Using an energy for self-diffusion of Q_{SD} = 2.06 eV [16], and a vacancy formation energy of E_v^f = 1.29 eV [17] leads to a vacancy migration energy of 0.77 eV. The low temperature self-diffusivity data [18,19] and Q_{SD} are then used in Eq. (1) to determine the entropy for self-diffusion, $S_v^m + S_v^f$ = 3.63 k. This entropy can then be broken into the migration and formation components by using a vacancy concentration of C_v = 190 ppm at 1075°C [20] and C_v^{eq} in Eq. (1). This results in S_v^m = 1.2 k and S_v^f = 2.4 k. For nickel, the self-diffusivity data are also fairly well known. The self-diffusion energy has been found to be 2.88 eV [21] which corresponds well with independent measurements of E_v^f = 1.8 [22] and E_v^m = 1.04 eV [23]. However, values for the entropies are uncertain. Using the formalism of Eq. (1) for the data of Maier et al. [21] yields $S_v^m + S_v^f$ = 5.27 k, but the division between the two entropies is unknown.

Reliable self-diffusion data for stainless steel are scarce. Rothman et al. [24] have used tracer diffusion techniques to examine the diffusivity of the major elements Fe, Ni and Cr in an alloy of approximately the same composition as the P7 examined here. Appreciable differences were found by Rothman et al. in the diffusivities of the alloy components for a given composition as well as variations with composition between the same components in different alloying systems. Care must therefore be exercised in using diffusivity data from one steel alloy system and applying it to another. Making use of Eq. (1) again and Rothman et al.'s data give the results listed in Table 2. The division of these sums into their individual components is again unknown. For the nucleation calculations, the division is made by assuming constant values of E_v^f and S_v^f for all components, but different values of E_v^m and S_v^m for each alloy component. The vacancy diffusivity is then determined as an average

$$D_v = \overline{D}_v = \sum_\chi C_\chi D_v^\chi \tag{2}$$

where C_χ is the fraction of χ in the alloy and

$$D_v^\chi = a^2 \upsilon_o \exp\left(\frac{S_v^m(\chi)}{k}\right) \exp\left(\frac{-E_v^m(\chi)}{kT}\right) \tag{3}$$

with $\upsilon_o = \frac{1}{a}\sqrt{\overline{E_v^m}/M}$; $\overline{E_v^m} = \sum_\chi C_\chi E_v^m(\chi)$.

The surface energies used in this study are less then the values tabulated by Murr [25] by a factor of 2-3. This must be done because steady state void nucleation rates are too low when surface energy values for clean sur-

faces are employed [26]. This implies that either some unknown impurity segregation occurs to the void embryo surface which reduces its surface energy, or that there exists gas such as hydrogen or helium in the metal that can pressurize the void embryo. Both affect the vacancy concentration in equilibrium with a void [27] containing x vacancies, i.e.

$$C_v^o(x) = C_v^{eq} \frac{r(x-1)}{r(x)} \frac{Z_v^o(x-1)}{Z_v^o(x)} \exp\left[\frac{\gamma^o(x) - \gamma^o(x-1) - P\Omega}{kT}\right] \quad (4)$$

by changing the surface energy $\gamma^o(x)$ and the gas pressure P. Here, the surface energy $\gamma^o(x)$ has been corrected for temperature and curvature, $\gamma \Rightarrow \gamma^o(r(x),T)$, according to Si-Ahmed and Wolfer [28]. The other factors in Eq. (4) are the void radius, r(x), and the void bias for vacancies, $Z_v^o(x)$. As the surface energy, γ, is decreased, the void nucleation rate increases dramatically, in particular at high temperatures. The reduction in the vacancy concentration in equilibrium with a void embryo as given by Eq. (4) leads to a slower vacancy re-emmission rate. Similarily if the embryo is pressurized, the nucleation rate also increases.

The void bias factors Z_i^o and Z_v^o are obtained from a shell model presented previously [4, 28, 29]. The shell model also implies that a segregation region exists around the void which has a different shear modulus and lattice parameter than the matrix. This difference need only be on the order of 0.002 - 0.03% for void nucleation to occur at the desired rate. The effect of increasing the difference in shear modulus or lattice parameter is to increase the void bias for vacancies and decrease the bias for interstitials. The sink averaged bias factor ratio, $\overline{Z}_I/\overline{Z}_V$, for void nucleation is taken to be 1.4

which is about halfway to the large void steady state swelling value calculated by Sniegowski and Wolfer [30].

Results

The experimental results from the copper alloy, nickel, and P7 stainless steel irradiations can be grouped into three broad categories based on the observed effect of excess interstitials on the void density. The three categories are a) voids observed, with the magnitude of the injected ion effect quantitatively determined, b) voids observed, but no observed suppression in void density, and c) no voids observed. Table 3 summarizes these results for the various conditions that were investigated. The lower homologous irradiation temperatures generally give rise to a greater void density suppression, in agreement with theory.

A. Copper Alloys

No void formation was observed in cold-worked plus aged copper alloys that were irradiated up to peak damage levels of 15 dpa (K = 0.3) at homologous temperatures of 0.5 - 0.6 Tm (400° - 550°C). Irradiation of an annealed (500°C, 1 hr) AMZIRC (Cu-Zr) alloy to the same fluence at 300°C resulted in a sparse distribution of large (~ 250-500 nm diameter) voids. The void density was estimated to be on the order of $10^{17}/m^3$. The few voids which were observed were preferentially found in the vicinity of large zirconium particles present in the damage region of the alloy. Figure 1 shows two voids observed in cross-section in the irradiated AMZIRC alloy.

The calculated void nucleation rate versus irradiation temperature for pure copper is shown in Fig. 2. The void nucleation rate without excess interstitials (ε_i = 0) is compared to the nucleation rate with an excess interstitial fraction corresponding to the peak damage region ($\varepsilon_i = 10^{-3}$).

The displacement rate was taken as 3×10^{-3} dpa/s (K = 0.3), which corresponds to the peak damage rate during the copper alloy irradiations. It can be seen that the steady-state nucleation theory predicts an absence of homogeneous void nucleation in copper for irradiation temperatures $\gtrsim$ 300°C, in agreement with the experimental observations. The effect of the injected interstitials on void nucleation is predicted to be negligible for temperatures $\gtrsim$ 150°C.

B. Nickel

The 14-MeV Ni ion irradiations of nickel at 425°C and 450°C (0.40 - 0.42 Tm) both show a suppression in the void number density in the peak damage region. Figure 3 shows the observed TEM depth-dependent void distribution for a nickel sample irradiated to a peak damage level of 2 dpa (K = 0.3) at 450°C. The reduction in void density in the injected ion region is clearly visible in this figure. The void number density versus depth for both the 425°C and the 450°C nickel samples is shown in Fig. 4. The maximum suppression occurs at a depth of 1.6 and 2.1 μm for the 425 and 450°C irradiation temperatures, respectively. The extent of the suppression region for the 425°C sample, 0.5 - 2.8 μm, is larger than that for the 450°C sample (1.0 - 2.6 μm). The void number density for the 425°C sample is less than the 450°C sample density in the suppression region.

The calculated void nucleation rate as a function of depth for a 14-MeV Ni ion irradiation of nickel is shown in Fig. 5. The 450°C sample is seen to have a lower nucleation rate than the 425°C sample except in the region of suppression. This result agrees with the experimentally observed void density (Fig. 4). The maximum suppression of void nucleation is predicted to occur at 2.2 μm. The widths of the calculated suppression regions for the 425°C and 450°C cases are 1.6 to 2.5 μm and 1.6 to 2.4 μm, respectively.

C. P7 Stainless Steel

The P7 stainless steel samples were irradiated at 400°, 500° and 650°C up to a peak damage level of 20 dpa (K = 0.3). Small voids (diameter $\lesssim$ 2 nm) were observed at the end of range in the 400°C sample. However, inconclusive results were obtained for the depth-dependent void density due to the small void size. A suppression effect on void number density was observed in the high fluence 500°C sample [20 dpa (K = 0.3) at the peak damage region] whereas the low fluence 500°C sample (4 dpa peak damage) and the high fluence 650°C sample (20 dpa peak damage) showed no suppression effect. The low fluence 500°C sample had voids 1-2 nm in diameter which are difficult to detect due to their small size. This gives a large measurement error which is believed to be the reason no suppression effect was observed. Figure 6 shows TEM micrographs spanning the damage region in the 500°C high fluence P7 sample. A small decrease in the void number density in the peak region is evident. The void number density versus depth for the high fluence 500°C and 650°C samples are shown in Fig. 7. For the 650°C data the decreasing void number density in the peak damage region results from the large voids (~ 200 nm diameter) in the bimodal distribution reducing the number of voids through coalescence. The two size classes found in the 650°C sample are believed to be the result of an oxygen effect as discussed elsewhere [9,10]. Experimentally, the maximum suppression at 500°C is centered at 2.4 μm, where the amount of suppression results in a void number density decrease by a factor of ~ 3. The width of the suppressed region is from 1.9 μm to 2.9 μm. There is no apparent suppression in the 650°C sample.

Figure 8 is a plot of the theoretical nucleation rate versus depth for 14-MeV Ni ion-irradiated P7. The 400°C calculations show a significant suppression effect centered at a depth of 2.4 μm and extending from 1.7 μm to 3.1 μm. The 500°C calculation shows a smaller suppression centered at 2.5 μm and extending from 1.8 μm to 2.8 μm. At 650°C, there is only a small overall reduction of the nucleation rate with no characteristic suppression dip. The calculated nucleation rate at 650°C is about seven orders of magnitude too low to account for the experimental results.

Discussion

The theoretical calculations and experimental results of this study are in good qualitative agreement on the magnitude of the suppression effect and its sensitivity to irradiation temperature. A quantitative comparison between experiment and theory shows differences which must be attributed to additional effects not yet incorporated in the theory, and to the complex interdependence of materials parameters in an irradiation environment. At "low" temperatures the discrepancies between theory and experiment concerning the amount and position of the suppression of void nucleation may be attributed mainly to diffusional spreading. At "high" temperatures, where the excess interstitial effect is unimportant, the discrepancy between theoretical void nucleation rate and experimental observations may be attributed to the effect of impurities in the metal. Both of these effects are discussed below. Whether an irradiation is at a "high" or "low" temperature is unique to the metal being investigated and depends on the vacancy mobility and the impurity content.

For the "low" temperature irradiated Ni specimens, the observed suppression was larger and closer to the surface than the theoretical calculations would predict (Figs. 4, 5). The 425 and 450°C nickel samples gave a maximum suppression at depths of 1.6 and 2.1 μm with the suppression extending over a width of 2.3 and 1.6 μm, respectively. The theoretical results in Ni give a maximum suppression at 2.2 μm with widths of 1.0 and 0.8 μm. The increased width of the suppression zone with lower temperatures is probably due to recombination mechanisms becoming more dominant, which in turn enhance the effect of injected ions on void suppression. The differences in the maximum suppression position and in the width of the suppression region are more difficult to explain. One possible explanation for this difference is diffusional spreading. This is more apparent when the P7 results are examined. The P7-500°C sample has a maximum experimental suppression at 2.4 μm which extends over 1 μm in width and this agrees with the 2.5 and 1 μm from the theoretical results (Figs. 7, 8). The P7 experimental results are much closer to the theoretical predictions than in the case of nickel. From the materials parameters in Table 1 (e.g., E_v^m, S_v^m) it is apparent that the vacancy mobility in P7 will be lower than in the nickel. Diffusional spreading, which has recently been shown to be important [31,32], will then be larger in nickel than in P7 due to the differences in the vacancy mobility. This results in a larger shift of the suppression maximum towards the front surface for Ni relative to P7. Another indication of the diffusional spreading differences between the two metals is seen by examining the end of range data. Comparing theoretical to experimental end of range for Ni and P7 gives 2.8 to 3.4 μm and 3.1 to 3.5 μm, respectively. The end of range diffusional spreading is larger for nickel, 0.6 μm, than for P7, 0.4 μm.

At "high" temperatures, when there is very little suppression, the lack of good correlation between theory and experiment could be due to the presence of impurities in the metal that are not properly accounted for in the nucleation model. The copper alloy, AMZIRC, at 300°C and the stainless steel P7 at 650°C are good examples of this point. For AMZIRC, the nucleation code is based on "pure" copper while the irradiated specimen is a commercial copper alloy. If the solutes and impurities in the alloy act as trapping sites for vacancies, then the vacancy mobility is effectively decreased [33]. This decrease in the mobility can be accounted for in the nucleation code by raising the vacancy migration energy. Figure 9 is a plot of the void nucleation rate versus temperature in copper when E_v^m = 0.87 eV, implying an energy of 0.1 eV for trapping [34]. Comparison of Figs. 2 and 9 shows that the decrease in vacancy mobility will shift the "high" temperature nucleation rate by 30°C. The overall nucleation rate at 300°C has risen by ~ 5 orders of magnitude to a value of $10^{11}/m^3$-s. The disparity between the theoretical rate of $10^{11}/m^3$-s and the experimental rate of ~ $10^{14}/m^3$-s is not considered to be significant since it occurs at the upper temperature limit for void nucleation. Also evident from Fig. 9 is that a reduction in vacancy mobility increases the suppression effect of the injected interstitials on void nucleation.

Many of the voids observed in AMZIRC (Cu-Zr) were in the vicinity of large zirconium precipitates. The extreme heterogeneity of the voids in the copper alloy indicates that special circumstances are required for their formation. These circumstances are only approximated in the steady-state nucleation code because the sink density and segregation effects are time and space averages. An additional increase of 0.05 eV in the trapping energy, a

small decrease of the surface energy (which would occur if impurities segregated to the void embryos), or a small decrease in the sink strength brings the calculated void nucleation into exact agreement with the AMZIRC experimental results.

The appropriate surface energy of voids is an unknown parameter, yet it has a pronounced effect on the nucleation rate. Oxygen in the P7 alloy could have migrated to a void embryo surface and reduced the surface energy, thereby increasing the nucleation rate dramatically [9,10]. Decreasing the surface energy or increasing the gas pressure has a similar effect on the void nucleation. Figure 10 shows the theoretical predictions of the void nucleation rate when the surface energy of P7 is reduced to 0.1 J/m^2. This change gives a nucleation rate at 650°C which is approximately equal to that observed. A surface energy of 0.1 J/m^2 is, however, unrealistically low, and some other effects such as vacancy trapping by impurities or gas stabilization of void embryos must also play a role.

At very high temperatures, the theoretical predictions are in agreement with experimental results. The copper alloys that were ion irradiated $\gtrsim$ 400°C did not produce any voids, which is in agreement with the theory (Figs. 2 and 9). One reason for this lack of void nucleation may be that the vacancy reemission rate from a void, which increases with temperature, is too high due to lack of gas stabilization of the voids. When combined with the high vacancy mobility, which lowers the vacancy supersaturation, it makes void nucleation very unlikely. These results then indicate that in the absence of impurities, the peak void swelling temperature for ion irradiation of copper alloys is probably below 300°C. In this context it is important to note that both AMZIRC and AMAX-MZC are manufactured under carefully controlled (oxygen-

free) environments using OFHC copper, which means a low content of gaseous impurities. Other experimental work on ion-irradiated copper by Glowinski [35] and Knoll [7] confirm that voids do not form in de-gassed copper. This contrasts with the published neutron irradiation data which show that voids form readily between 220 and 550°C (0.35 - 0.60 Tm) [36]. Clearly, more research is required on the effect of gas on void nucleation in copper.

The suppression effect of the injected interstitials on void nucleation need not be limited to low temperatures. The presence of impurities and or gas in the metal may shift the start of the point defect recombination regime to higher temperatures. The use of low energy ($\lesssim$ 5 MeV) self-ions to irradiate the metal would exacerbate such a temperature shift because the excess interstitial fraction, and hence the suppression effect, increases with decreasing ion energy [3,5]. For 14-MeV compared to 5-MeV Ni ions on nickel, the excess interstitial fraction increases from 3×10^{-3} to 6×10^{-3} where both of these values correspond to the ion deposition peak and K = 0.3 [3].

The combination of impurities and/or gas with a low energy self-ion irradiation of a metal is illustrated by the following cases. Johnston et al. [37] found an extensive mid-range suppression in the void density for 5-MeV Ni ion irradiated stainless steel at 625°C. Farrell et al. [32] observed a mid-range suppression in the void density of nickel dual-irradiated with helium and 4-MeV Ni ions at 600°C. These observed suppression effects occurred at temperatures much higher than expected from self-ion irradiation results presented here and elsewhere [6]. The impurities (or solutes) in the steel and the implanted gas (and/or impurities) in the nickel may have trapped the point defects in such a manner as to cause recombination to dominate the point defect loss mechanisms. This would make the excess interstitials a larger

fraction of the point defects going to sinks (e.g. voids) and would result in reduced void nucleation. The above indicates that any void swelling results obtained from the peak damage region must be used with caution.

Conclusions

The following general conclusions may be drawn concerning void formation in ion-irradiated metals. These conclusions are currently valid only when applied to nickel, copper and stainless steel but may be more broadly applicable to all metals.

1. Qualitative agreement between theory and experiment regarding void nucleation in the presence of injected ions is very good. The injected ion effect becomes important as the irradiation temperature is decreased. The actual temperature where the effect becomes significant depends on the metal being investigated and on the impurity and/or gas content of that metal.
2. Quantitative agreement between theory and experiment regarding the effect of injected ions on void nucleation is fair. It appears that the discrepancies are due to neglect of diffusional spreading and impurity effects in the nucleation theory.
3. The magnitude of void nucleation suppression can be very significant below certain temperatures. Void swelling data from ion irradiations should not be taken from the peak damage region when experimental conditions exist which make the injected ion effect important.
4. As is evident from ion irradiation studies on pure copper and copper alloys, the relative temperature regime for swelling is determined by the vacancy mobility, not by the melting point of the metal, i.e. the void swelling regime is not necessarily 0.35 - 0.6 Tm.

Acknowledgements

The authors gratefully acknowledge the support of the Department of Energy, Office of Fusion Energy. We would also like to thank D.B. Bullen for preparation of the nickel samples used in this study.

References

[1] Brailsford, A.D. and Mansur, L.K., J. Nucl. Mat. 71 (1977) 110.

[2] Lee, E.H., Mansur, L.K. and Yoo, M.H., J. Nucl. Mat. 85 & 86 (1979) 577.

[3] Plumton, D.L. and Wolfer, W.G., J. Nucl. Mat. 120 (1984).

[4] Garner, F.A., J. Nucl. Mat. 117 (1983) 177.

[5] Plumton, D.L., Attaya, H. and Wolfer, W.G., "Conditions for the Suppression of Void Formation During Ion-Bombardment," Third Topical Meeting on Fusion Reactor Materials, Albuquerque, NM, 19-23 Sept. 1983.

[6] Whitley, J.B., Kulcinski, G.L., Wilkes, P. and Smith Jr., H.V., J. Nucl. Mat. 7 (1979) 159.

[7] Knoll, R.W., "Effects of Heavy Ion Irradiation on the Phase Stability of Several Copper-Base Alloys," Ph.D. Thesis, Nuclear Engineering Department, University of Wisconsin-Madison (UWFDM-436).

[8] Shiraishi, K., Tanaka, M.P., Aruga, T. and Hamada, S., ASTM STP 782 (1982) pp. 927-940.

[9] Sindelar, R.L., Kulcinski, G.L. and Dodd, R.A., "Depth Dependent Microstructure of Ion-Irradiated Type 316 Stainless Steel," Third Topical Meeting on Fusion Reactor Materials, Albuquerque, NM, Sept. 19-23, 1983.

[10] Sindelar, R.L., Dodd, R.A. and Kulcinski, G.L., "A Comparison of the Depth-Dependent Microstructure of Ion-Irradiated 316-Type Stainless Steels," Proc. 12th International Symposium on the Effects of Radiation on Materials, 18-20 June 1984, Williamsburg, VA.

[11] Zinkle, S.J., Dodd, R.A. and Kulcinski, G.L., "Comparison of Thermal and Irradiated Behavior of High-Strength, High Conductivity Copper Alloys," Proc. 12th International Symposium on the Effects of Radiation on Materials, 18-20 June 1984, Williamsburg, VA.

[12] Torrens, I.M. and Robinson, M.T., Radiation Induced Voids in Metals, J.W. Corbett and I.C. Ianniello, Eds. (1972) 739.

[13] Kinney, J.H., Guinan, M.W. and Munir, Z.A., Presented at the Third Topical Meeting on Fusion Reactor Materials, Albuquerque, NM, Sept. (1983).

[14] Brice, D.K., Sandia National Laboratory Report SAND 75-0622 (1977).

[15] Seeger, A. and Mehrer, H., Vacancies and Interstitials in Metals, ed. by A. Seeger, D. Schumacher, W. Schilling and J. Diehl, North Holland, Amsterdam, 1970, p. 1.

[16] Bourassa, R.R. and Leugeler, B., J. Phys. F: Metal Phys. 6 (1976) 1405.

[17] Triftshäuser, W. and McGervey, J.D., Appl. Phys. 6 (1975) 177.

[18] Maier, K., Bassani, C. and Schule, W., Phys. Lett. 44A (1973) 539.

[19] Lam, N.Q., Rothman, S.J. and Nowicki, L.J., Phys. Stat. Sol. (9) 23 (1974) K35.

[20] Simmons, R.O. and Balluffi, R., Phys. Rev. 129 (1963) 1533.

[21] Maier, K., Mehrer, H. Lessmann, E. and Schule, W., Phys. Stat. Sol. 78 (1976) 689.

[22] Smedskjaer, L.C., Fluss, M.J., Legnini, D.G., Chason, M.K. and Siegel, R.W., J. Phys. F: Metal Phys. 11 (1981) 2227.

[23] Khana, S.K. and Sonnenberg, K., Rad. Effects 59 (1981) 91.

[24] Rothman, S.J., Noicki, L.J. and Murch, G.E., J. Phys. F: Metal Phys. 10 (1980) 383.

[25] Murr, L.E., Interfacial Phenomena in Metals and Alloys, Addison-Wesley, Reading, MA (1975).

[26] Wolfer, W.G. and Yoo, M.H., in "Radiation Effects and Tritium Technology for Fusion Reactors," Gatlinburg, TN (1976), Vol. II, CONF-750989.

[27] Katz, J.L. and Wiedersich, H., J. Chem. Phys. 55 (1971) 1414.

[28] Si-Ahmed, A. and Wolfer, W.G., ASTM STP 783 (1982) 1008.

[29] Wolfer, W.G. and Mansur, L.K., J. Nucl. Mat. 91 (1980) 265.

[30] Sniegowski, J.J. and Wolfer, W.G., "On the Physical Basis for the Swelling Resistance of Ferritic Steels," Topical Conf. on Ferritic Alloys for Use in Nuclear Energy Technologies, Snowbird, UT, USA, 19-23 June 1983.

[31] Mansur, L.K. and Yoo, M.H., J. Nucl. Mat. 85 & 86 (1979) 523.

[32] Farrell, K. Packan, N.H. and Houston, J.T., Rad. Effects 62 (1982) 39.

[33] Garner, F.A. and Wolfer, W.G., J. Nucl. Mat. 102 (1981) 143-150.

[34] Doyama, M., J. Nucl. Mat. 69 & 70 (1978) 350.

[35] Glowinski, L.D. and Fiche, C., J. Nucl. Mat. 61 (1976) 22.

[36] Knoll, R.W., "A Literature Review of Radiation Damage Data for Copper," University of Wisconsin Fusion Engineering Program Report UWFDM-384 (Oct. 1980).

[37] Johnston, W.G., Rosolowski, J.H., Turkalo, A.M., Lauritzen, T., J. Nucl. Mat. 62 (1976) 167.

[38] Cullity, B.D., "Elements of X-Ray Diffraction," 2nd Ed., Addision-Wesley, Reading, MA (1978) pp. 506-508.

[39] Hirth, J.P. and Lothe, J., "Theory of Dislocations," 2nd Ed., John Wiley & Sons, New York (1982) p. 837.

[40] Dieter, G.E., "Mechanical Metallurgy," 2nd Ed., McGraw-Hill, New York (1976) p. 51.

[41] Ehrhart, P., Conf. on Dimensional Stability and Mechanical Behavior of Irradiated Metals and Alloys, BNES, London, 1983, paper 17.

[42] Robrock, K.H., Conf. on Dimensional Stability and Mechanical Behavior of Irradiated Metals and Alloys, BNES, London, 1983, paper 18.

[43] Theis, U. and Wollenberger, H., J. Nucl. Mat. 88 (1980) 121.

Table 1. Materials Parameters

Parameter	Ni	Cu	P7	Reference
Lattice parameter, a_o (nm)	0.352	0.361	0.356	[38]
Surface energy, γ_o (J/m^2)	0.8	0.8	0.8	
Shear modulus, μ (MPa)	9.47×10^4	4.1×10^4	6.55×10^4	[39,40]
Poisson's ratio, ν	0.28	0.33	0.28	[39,40]
Vacancy formation energy[a], E_v^f	1.84	1.29	1.82	see text
Vacancy migration energy[a], E_v^m	1.04	0.77	1.29 (Ni) 1.38 (Cr) 1.39 (Fe)	see text
Pre-exponential factor, (m^2/s) $D_{vo} = a_o^2 \nu_o e^{S_v^m/k}$	4×10^{-6}	1.3×10^{-6}	---	
Mass of diffusing atom, M (amu)	58.7	63.5	56	
Vacancy formation entropy[b], S_v^f	3.0	2.4	2.5	see text
Vacancy migration entropy[b], S_v^m	2.3	1.2	3.1 (Ni) 4.3 (Cr) 4.8 (Fe)	see text
Interstitial relaxation volume[c], v_I	1.8	1.55	1.8	[41]
Vacancy relaxation volume[c], v_v	-0.2	-0.1	-0.1	[30]
Interstitial polarizability[a], α_I^G	72	34	52	[42]
Vacancy polarizability[a], α_v^G	39	18	28	[42]
Modulus variation, $\Delta\mu/\mu$	2×10^{-5}	3×10^{-4}	4×10^{-5}	
Lattice parameter variation, $\Delta a_o/a_o$	2×10^{-5}	3×10^{-4}	4×10^{-5}	
Cascade survival fraction, η	0.15	0.15	0.15	[43]
Sink strength, S (m^{-2})	5×10^{13}	10^{14}	10^{14}	
Bias factor ratio, $\bar{Z}_I/\bar{Z}_v$	1.4	1.4	1.4	see text
Thickness of segregation shell, h/r	0.1	0.1	0.1	

[a] In units of eV

[b] In units of the Boltzmann constant k

[c] In units of the atomic volume $\Omega = a_o^3/4$

Table 2. Self-Diffusion Data in a Steel Alloy

Component	$S_v^m + S_v^f$	$E_v^m + E_v^f$
17% Ni	5.58 k	3.11 eV
17% Cr	6.85 k	3.2 eV
66% Fe	7.3 k	3.21 eV

Table 3. Experimental Results

Material	Temperature	T/T_m	Peak Dose (dpa) *	Suppression Results
Cu Alloys	300°C	0.42	15	Inconclusive
	400°C	0.50	15	No voids
	500°C	0.57	15	No voids
	550°C	0.61	15	No voids
Ni	425°C	0.40	2	Suppression
	450°C	0.42	2	Suppression
P7	400°C	0.40	20	Inconclusive
	500°C	0.45	4,20	Suppression
	650°C	0.54	20	No suppression

*Displacement efficiency K = 0.3

Figure Captions

Fig. 1. Cross-section TEM micrograph showing voids in annealed AMZIRC irradiated with 14-MeV Cu ions to a peak damage level of 15 dpa (K = 0.3) at 300°C.

Fig. 2. Theoretical void nucleation rate vs. temperature in Cu at a damage rate of 3×10^{-3} dpa/s with $E_v^m = 0.77$ eV.

Fig. 3. Depth-dependent void microstructure of nickel irradiated with 14-MeV Ni ions to a peak damage level of 2 dpa (K = 0.3) at 450°C. Note the absence of voids in the implanted ion region.

Fig. 4. Experimentally observed void density as a function of depth for nickel following 14-MeV Ni ion irradiation at 425°C and 450°C to peak damage levels of 2 dpa (K = 0.3).

Fig. 5. Theoretical void nucleation rate vs. depth for 14-MeV Ni on Ni at 425°C and 450°C. Dashed line corresponds to no injected ions ($\varepsilon_i = 0$). Solid line uses ε_i from Brice [14].

Fig. 6. Depth-dependent void microstructure of P7 irradiated with 14-MeV Ni ions to a peak damage level of 20 dpa (K = 0.3) at 500°C.

Fig. 7. Experimentally observed void density as a function of depth for P7 following 14-MeV Ni ion irradiation at 500°C and 650°C to peak damage levels of 20 dpa (K = 0.3).

Fig. 8. Theoretical void nucleation rate vs. depth for 14-MeV Ni on P7 at 400, 500 and 650°C assuming $\gamma = 0.8$ J/m^2. Dashed line is $\varepsilon_i = 0$, solid line is ε_i from Brice [14].

Fig. 9. Comparison of the theoretical void nucleation rate vs. temperature in Cu at a damage rate of 3×10^{-3} dpa/s with and without a vacancy binding energy of 0.1 eV.

Fig. 10. Theoretical void nucleation rate vs. depth for 14-MeV Ni on P7 at 400, 500 and 650°C assuming $\gamma = 0.1$ J/m^2. Dashed line is $\varepsilon_i = 0$, solid line is ε_i from Brice [14].

FIGURE 1

VOIDS IN IRRADIATED AMZIRC

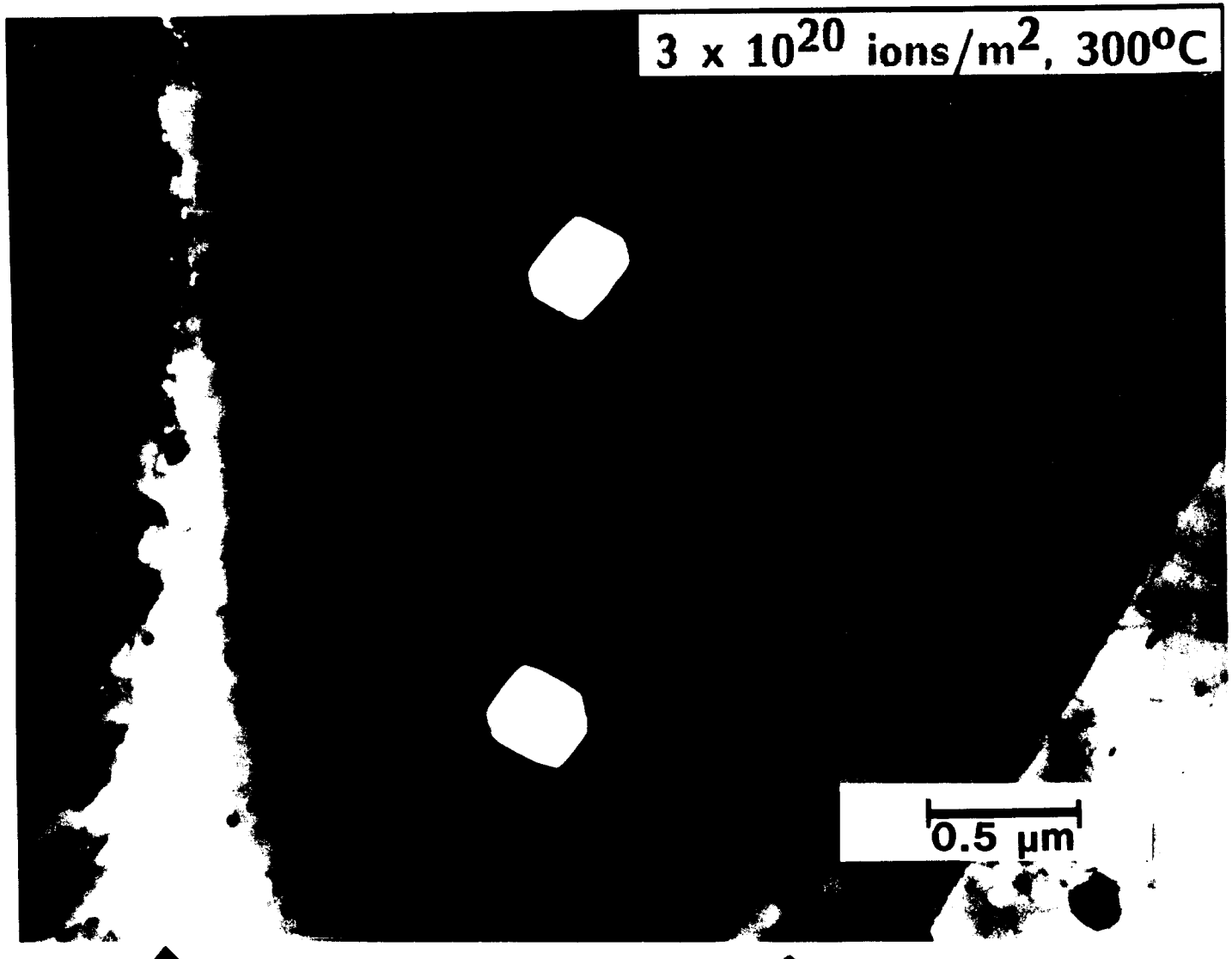

FIGURE 2

CALCULATED VOID NUCLEATION RATE IN THE PEAK DAMAGE REGION FOR 14 MeV Cu on Cu

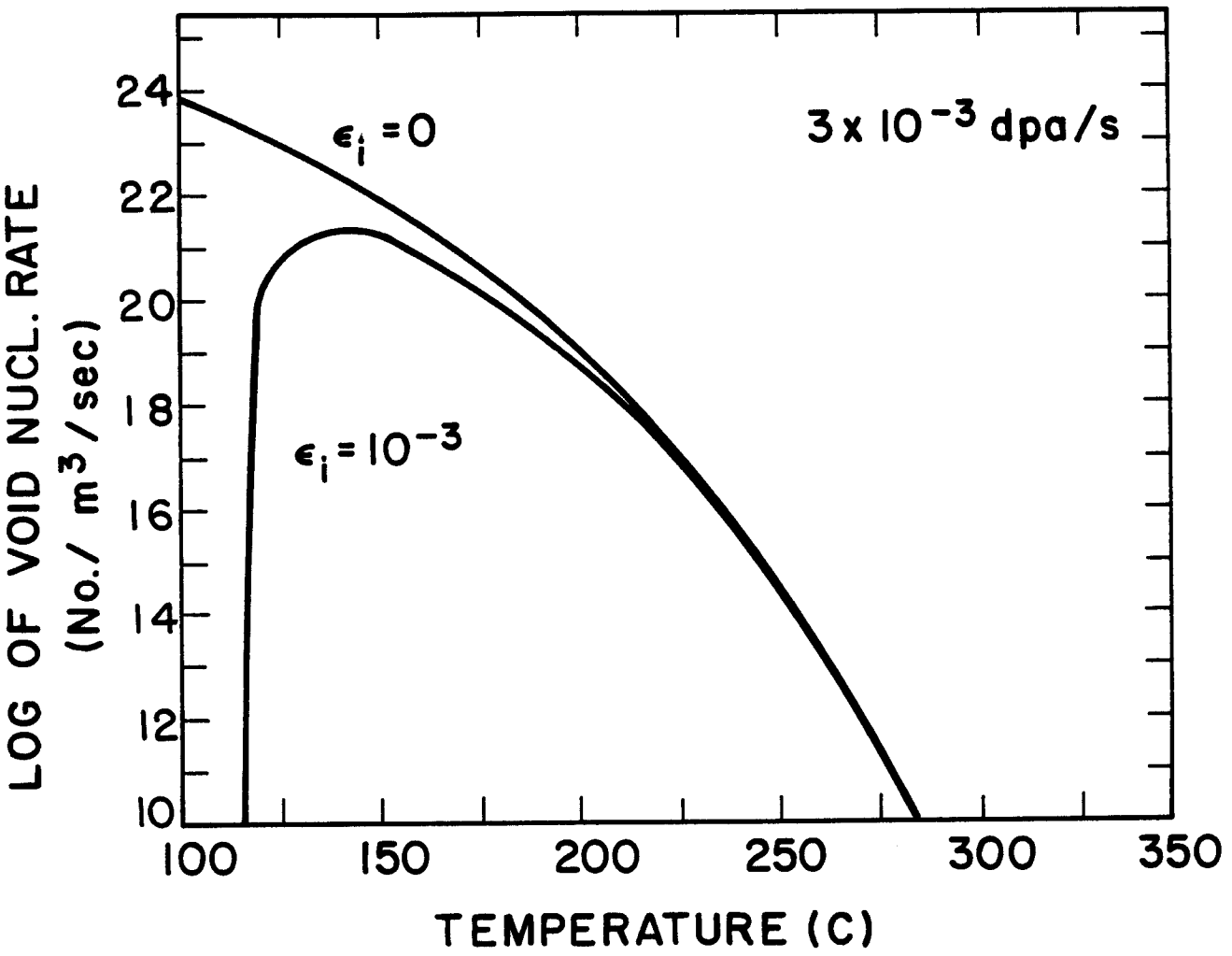

FIGURE 3

VOID SUPPRESSION IN NICKEL DUE TO INJECTED INTERSTITIALS

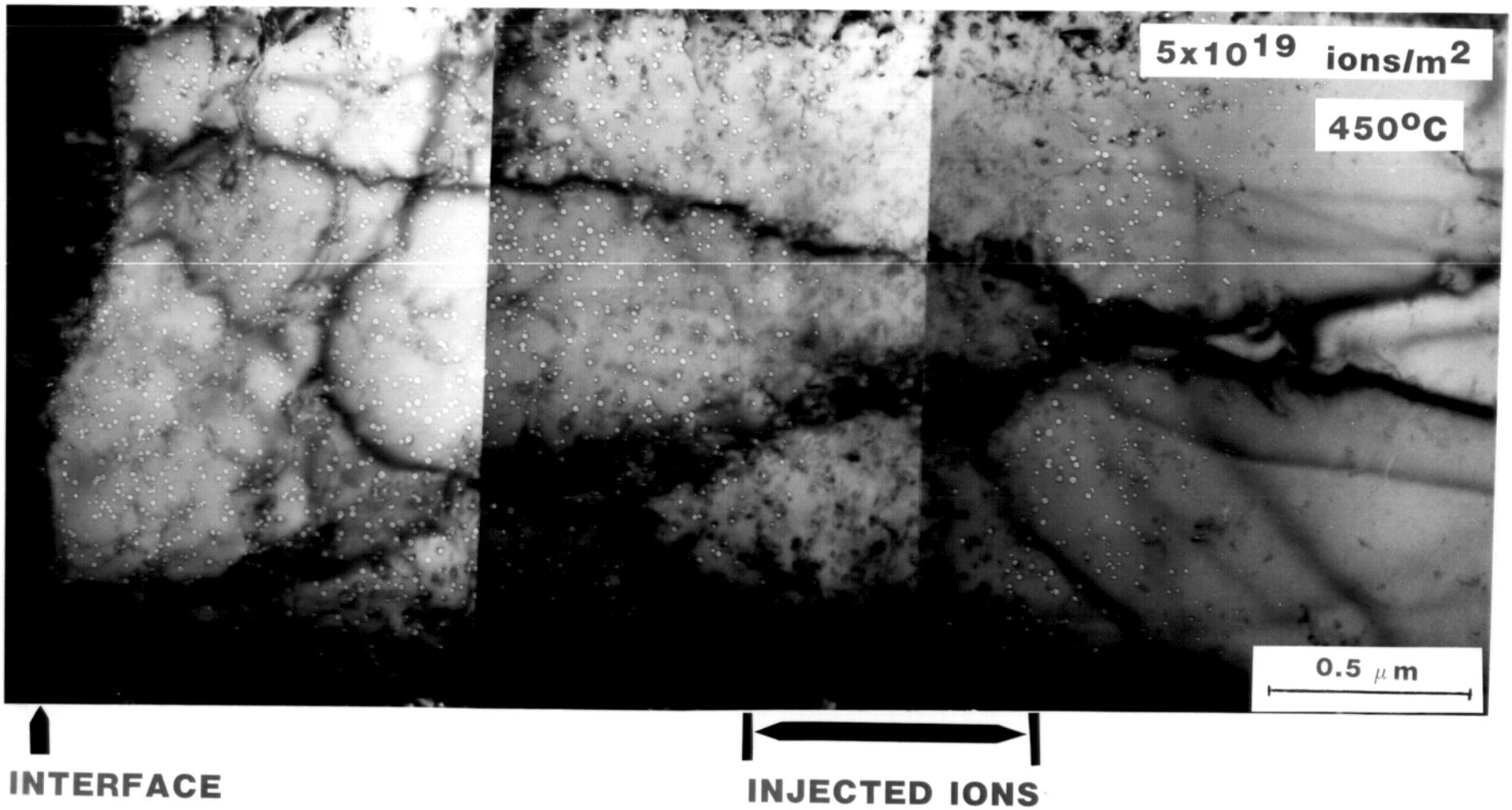

FIGURE 4

Experimentally Observed
Depth-Dependent Void Number Density
For 14 MeV Ni on Ni

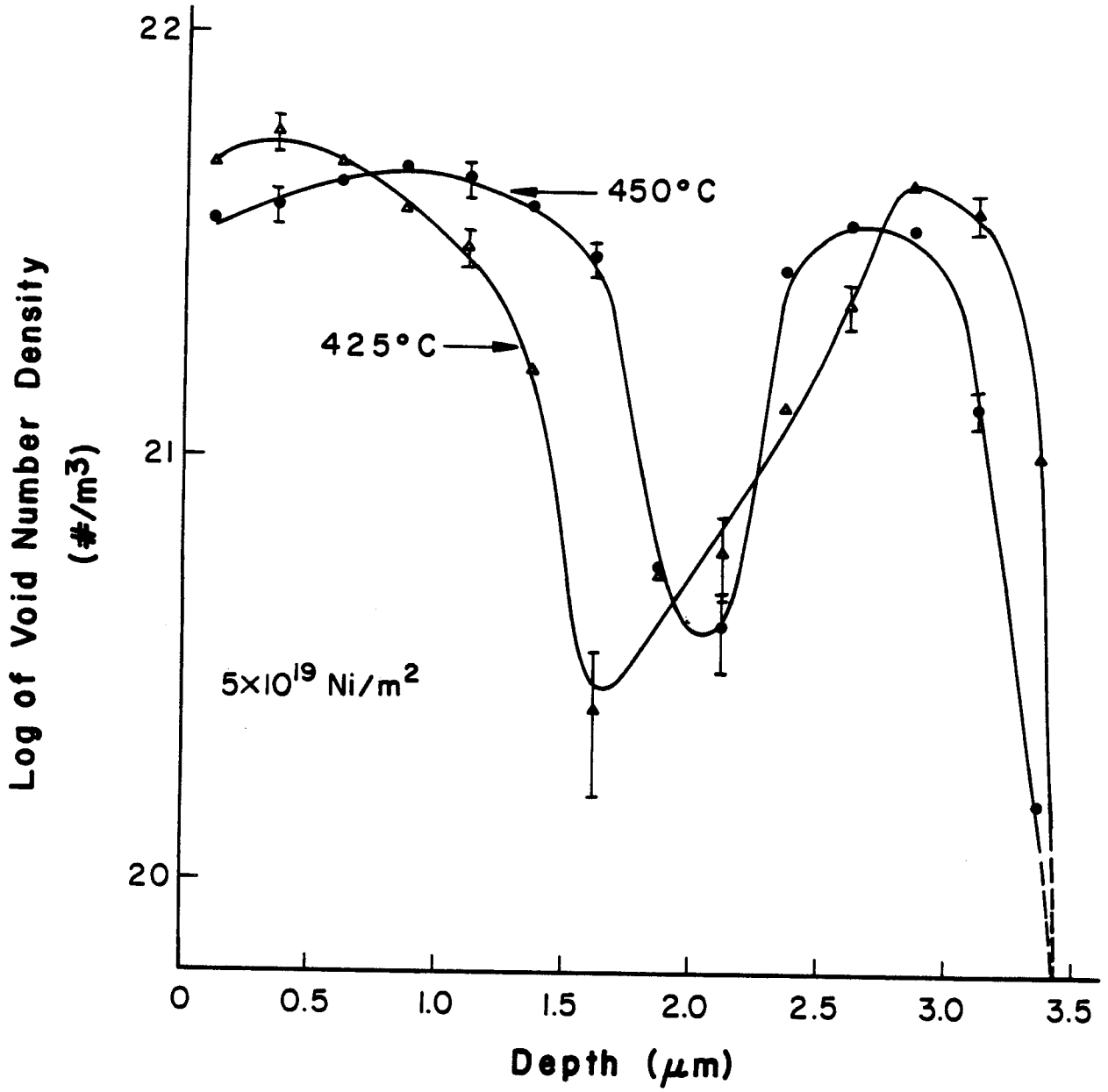

FIGURE 5

Calculated Depth-Dependent
Void Nucleation Rate
For 14 MeV Ni on Ni

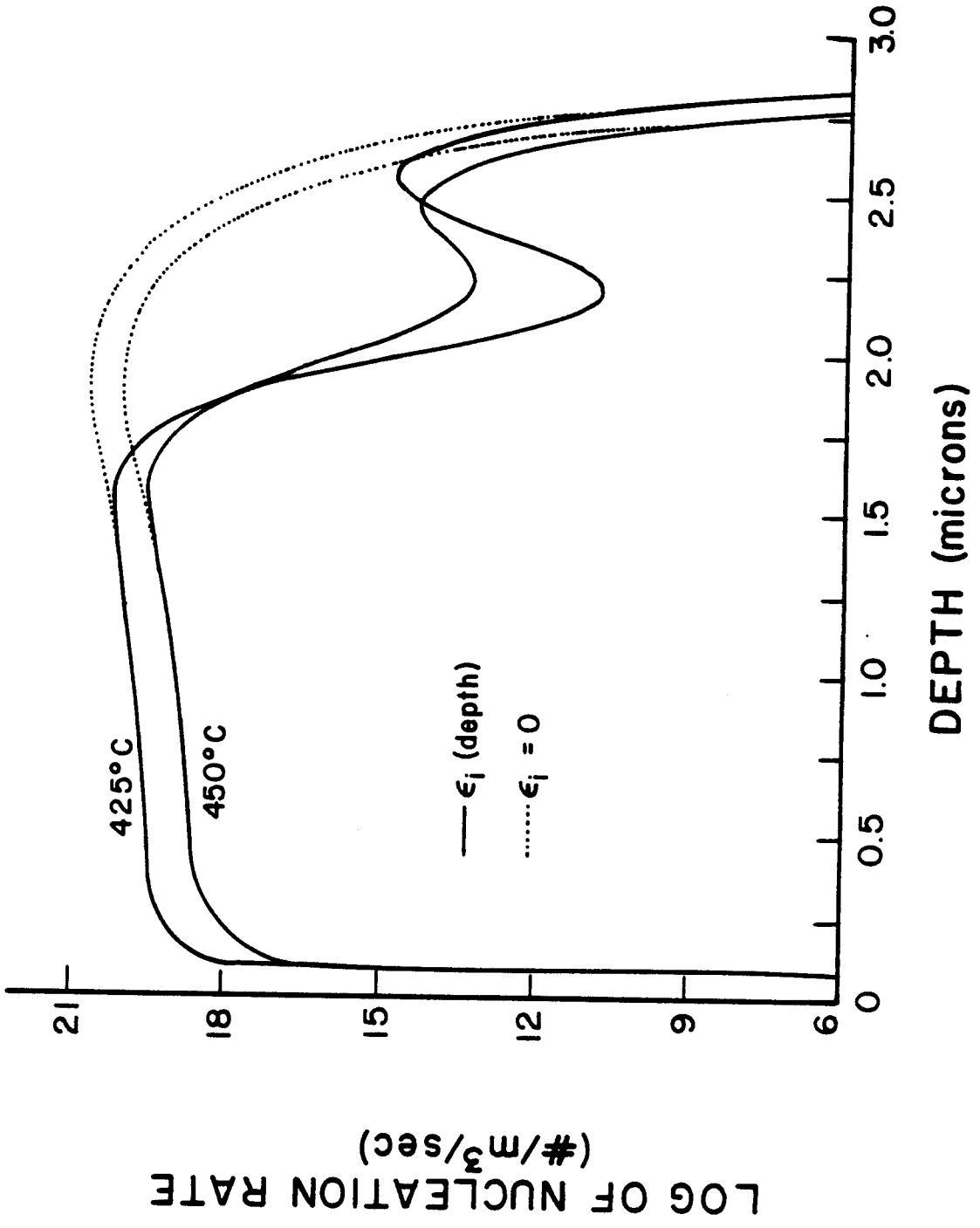

FIGURE 6

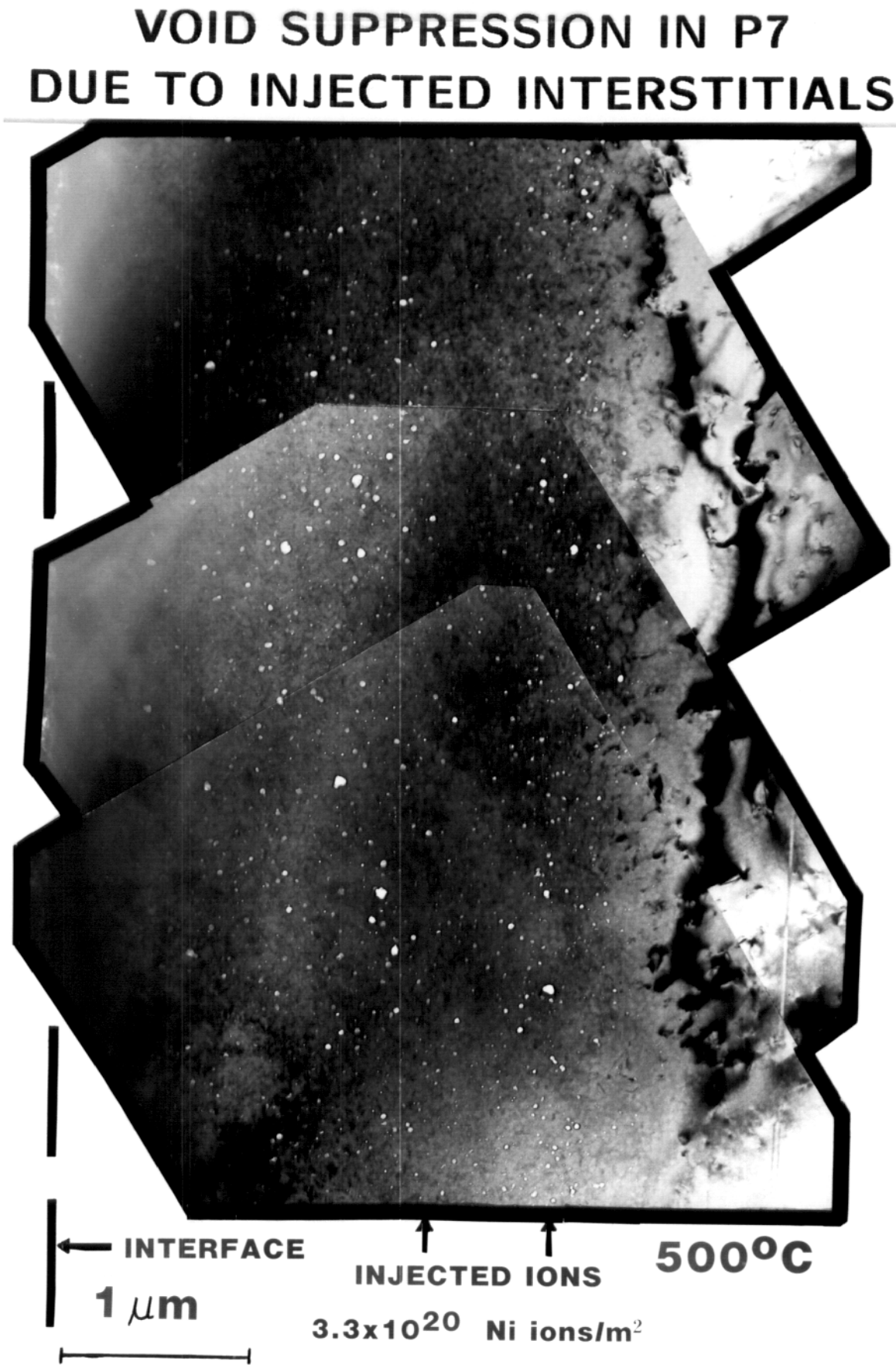
VOID SUPPRESSION IN P7
DUE TO INJECTED INTERSTITIALS
INTERFACE
INJECTED IONS
500°C
1 μm
3.3x10^20 Ni ions/m^2

FIGURE 7

Experimentally Observed
Depth-Dependent Void Number Density
For 14 MeV Ni on P7

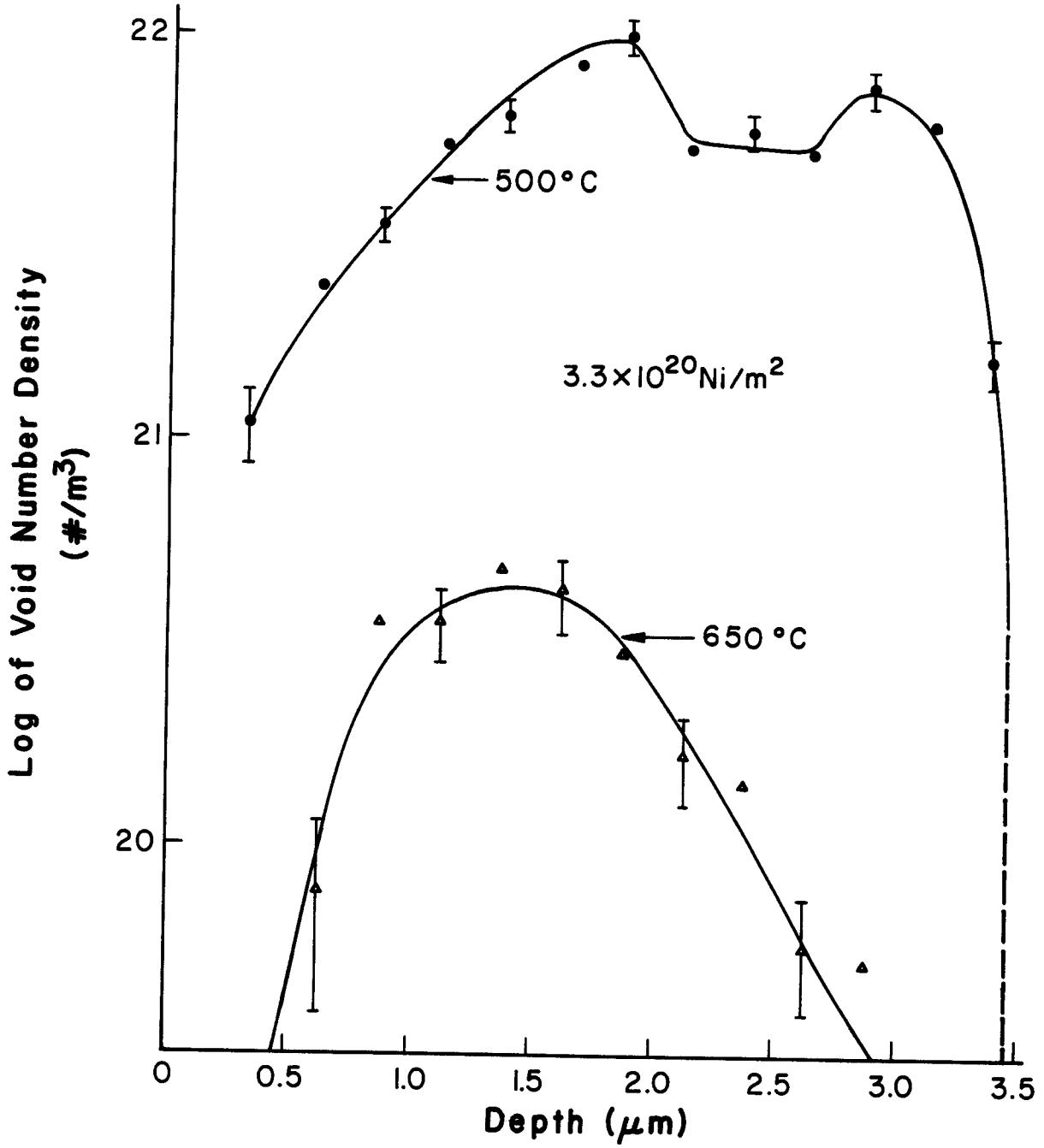

FIGURE 8

Calculated Depth-Dependent Void Nucleation Rate For 14 MeV Ni on P7

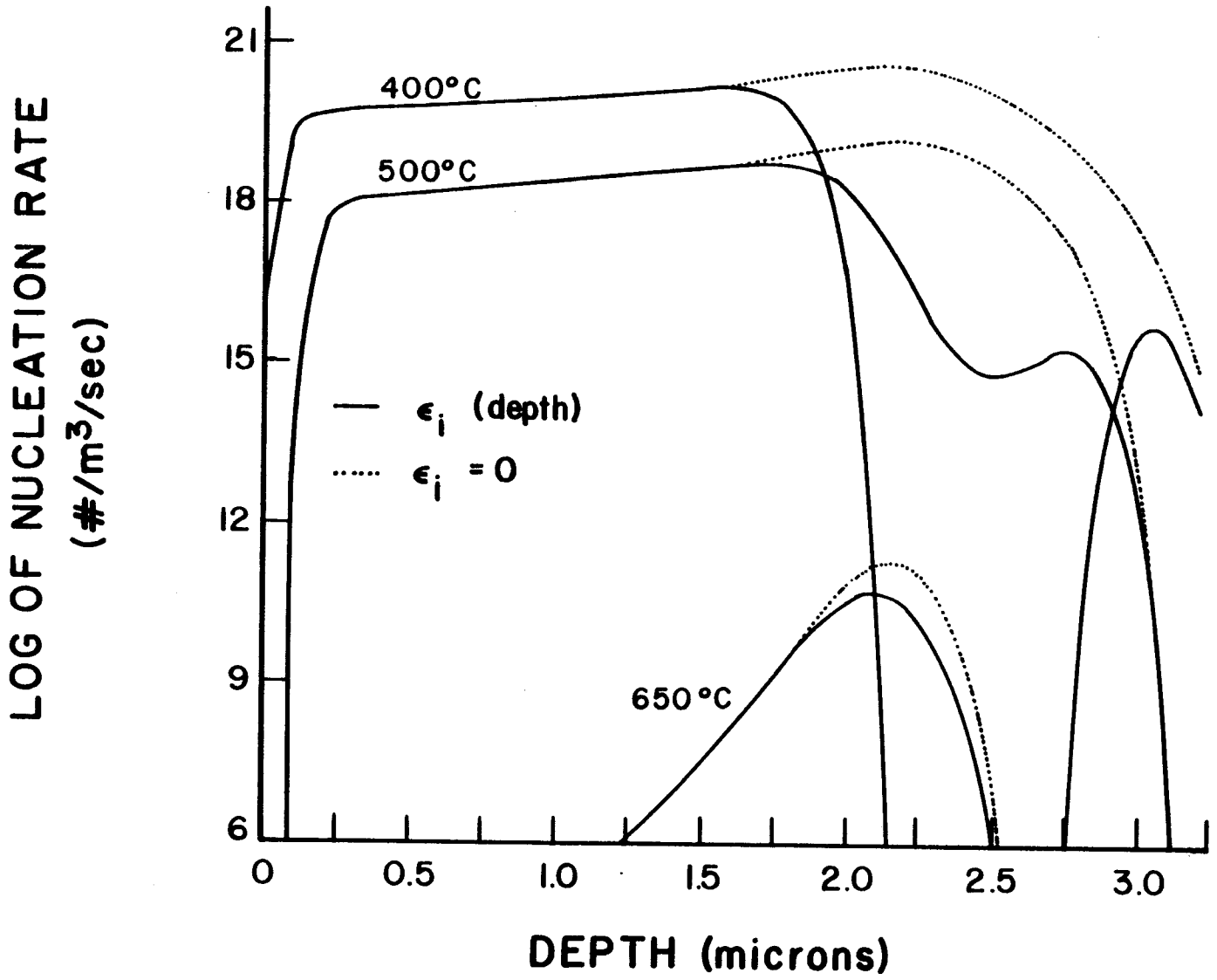

FIGURE 9

CALCULATED VOID NUCLEATION RATE IN THE PEAK DAMAGE REGION FOR 14 MeV Cu on Cu

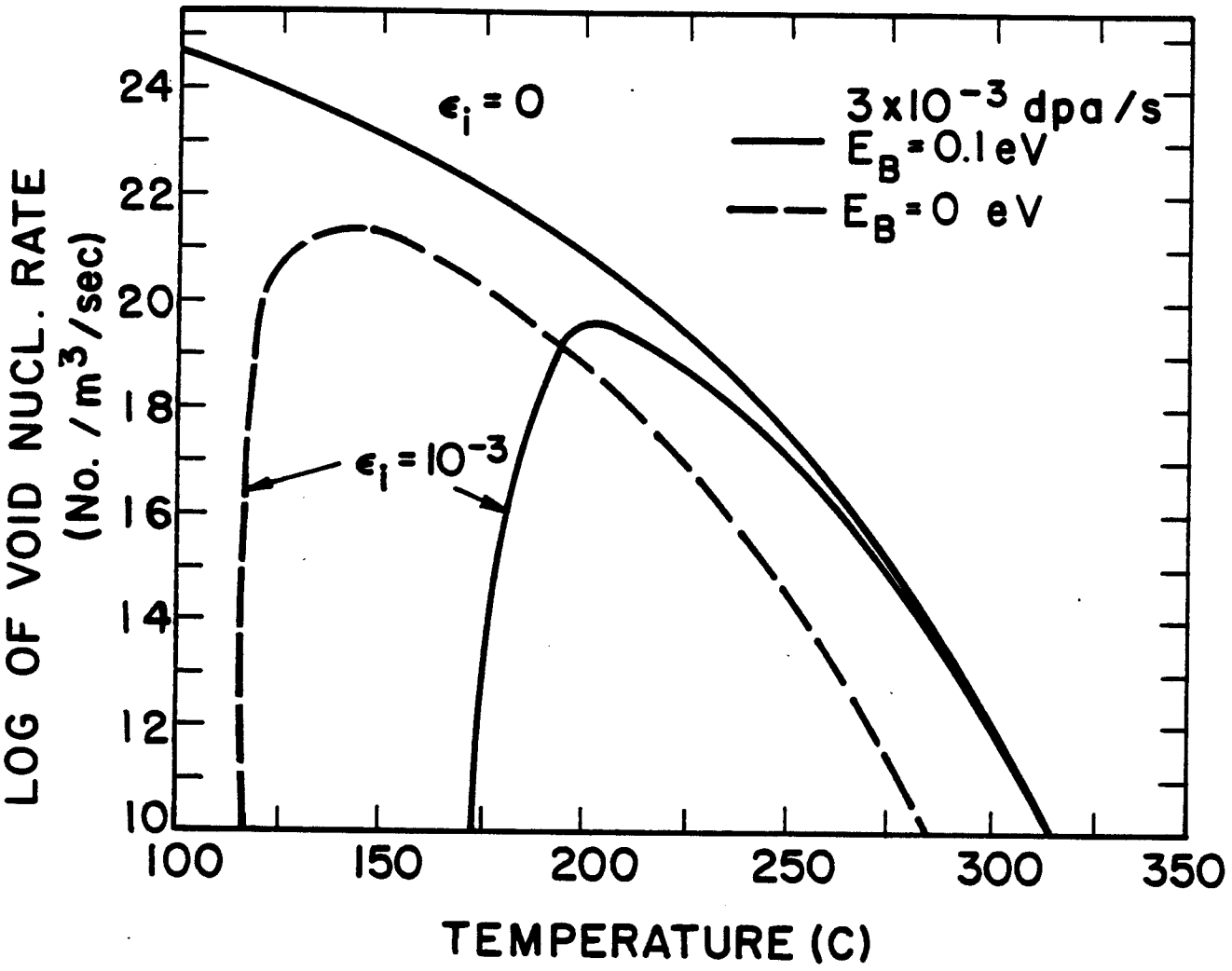

FIGURE 10

Calculated Depth-Dependent
Void Nucleation Rate
For 14 MeV Ni on P7